Tuning the Primary Reaction of Channelrhodopsin-2 by Imidazole, pH, and Site-Specific Mutations

Frank Scholz,[†] Ernst Bamberg,[‡§] Christian Bamann,[‡] and Josef Wachtveitl[†*]
[†]Institute of Physical and Theoretical Chemistry and [§]Institute of Biophysical Chemistry, Johann Wolfgang Goethe-University, Frankfurt/Main, Germany; and [‡]Max Planck Institute of Biophysics, Frankfurt/Main, Germany

ABSTRACT Femtosecond time-resolved absorption measurements were performed to investigate the influence of the pH, imidazole concentration, and point mutations on the isomerization process of Channelrhodopsin-2. Apart from the typical spectral characteristics of retinal isomerization, an additional absorption feature rises for the wild-type (wt) on a timescale from tens of ps to 1 ns within the spectral range of the photoproduct and is attributed to an equilibration between different K-intermediates. Remarkably, this absorption feature vanishes upon addition of imidazole or lowering the pH. In the latter case, the isomerization is dramatically slowed down, due to protonation of negatively charged amino acids within the retinal binding pocket, e.g., E123 and D253. Moreover, we investigated the influence of several point mutations within the retinal binding pocket E123T, E123D, C128T, and D156C. For E123T, the isomerization is retarded compared to wt and E123D, indicating that a negatively charged residue at this position functions as an effective catalyst in the isomerization process. In the case of the C128T mutant, all primary processes are slightly accelerated compared to the wt, whereas the isomerization dynamics for the D156C mutant is similar to wt after addition of imidazole.

INTRODUCTION

Almost ten years ago, Channelrhodopsins were first described as light-gated cation channels (1,2). Later studies showed that Channelrhodopsin-2 (ChR2) also pumps protons across a cell membrane; it was then termed a "leaky proton pump" (3). The possibility to control an ion channel through light stimulation was widely used to selectively depolarize cell membranes leading to the firing of action potentials (4,5). Together with its counterpart the chloride pump halorhodopsin, these proteins became excellent tools in the emerging scientific field of optogenetics (6). Despite the ongoing research concerning optogenetic applications, relatively little is known about the molecular mechanisms of ChR2.

Recently, the crystal structure of a C1C2 chimera between ChR1 and ChR2 was reported, exhibiting an overall molecular architecture similar to bacteriorhodopsin (bR), with retinal covalently bound through a Schiff base with a lysine residue to the protein (7). A 6 Å-projection map obtained by cryo-electron microscopy indicates the existence of ChR2 as a stable dimer (8). Retinal extraction experiments and resonance Raman spectroscopy reveal a mixture of all-*trans* and 13-*cis* conformations (70:30) in dark-adapted ChR2 (9). Recently, the primary photodynamics for the ChR2 wt at pH 7.4 was investigated using femtosecond time-resolved absorption spectroscopy (10). Photoexcitation triggers an isomerization around the C13-C14 double bond leading to the formation of a ground-state photointermediate (K-like intermediate). The primary photodynamics exhibits a high similarity to sensory rhodopsin II (NpSRII) (11) and bR (12,13). Therefore, the driving forces catalyzing the isomerization, e.g., the hydrogen-bond network and electrostatic interactions, are assumed to be similar. Like in other retinal proteins, the *trans-cis* isomerization around the C13-C14 double bond induces a photocycle consisting of a series of thermally driven reaction intermediates (14,15).

The primary processes occurring on a picosecond timescale are decisive for the quantum efficiency of the protein. A part of the population in the excited state relaxes back to the initial ground state without isomerization. The branching point between the reactive and the unreactive pathway is located before reaching the K-like intermediate.

In this study, we first probed the proximate vicinity of the protonated Schiff-base. The Schiff-base proton is stabilized by a water-mediated network of hydrogen bonds (9) and the counterion, consisting presumably of R120, D253, and E123 (Fig. 1). Early reports proposed E123 as primary proton acceptor (14,16), whereas the recently published crystal structure of a C1C2 chimera assigned this function to D253 (7). Both residues provide protonation sites in close vicinity to the retinal. Hence, the electrostatic environment is altered upon lowering the pH and thereby neutralizing these negatively charged residues. Because the excited state of retinal is supposed to exhibit a charge-transfer character, the isomerization dynamics should be pH-dependent. Therefore, these experiments provide information about the response of the retinal after photoexcitation in an altered environment. Furthermore, we investigated the isomerization dynamics in mutations where E123 was replaced by a neutral (E123T) and a negatively charged amino-acid residue (E123D), respectively. Recently it was shown that these mutations of E123 influence the spectral and

Submitted November 14, 2011, and accepted for publication April 19, 2012.

*Correspondence: wveitl@theochem.uni-frankfurt.de

Editor: Petra Schwille.

0006-3495/12/06/2649/9 $2.00

doi: 10.1016/j.bpj.2012.04.034

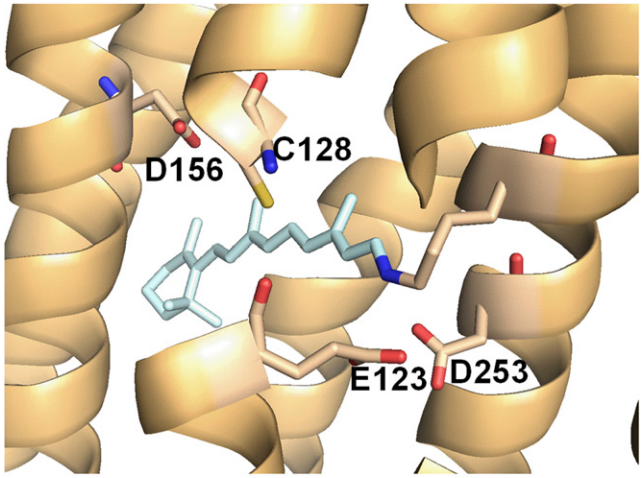

FIGURE 1 Retinal binding pocket of ChR2 based on the crystal structure of a C1C2 chimeras (PDB access code: 3UG9).

photocycle properties of ChR2, while retaining the channel function (17).

While the proton concentration and the E123X mutations affect the charge of acidic side chains, we tested other means to modulate the hydrogen-bonding network and its impact on the isomerization. Imidazole, like azide, is a weak proton donor and either acts as proton shuttle between the vicinity of the Schiff base and the external aqueous bulk phase (18) or interacts with the hydrogen-bonding network of the protein (19). Therefore, imidazole effects on the kinetics of ChR2 provide information on the primary reaction steps with an altered hydrogen-bonding network.

We also tried to address the coupling of the primary photoreaction to the late stages of the photocycle that are connected with the gating of the channel. For bR, it is well established that T90 forms a hydrogen bond with D115 stabilizing the structure of helix C. Mutations of T90 affect the proton transport efficiency and the photocycle kinetics (20). Strong evidence comes from vibrational spectroscopy that this internal hydrogen bond is also present in ChR2 between the corresponding amino acids C128 and D156 (21). Point mutations of these two amino acids lead to a longer open state of the channel that can last for tens of seconds to even minutes (16,22). It was thus supposed that this hydrogen bond plays a central role in the gating of the channel (16,21,22). This element differs in the recently published crystal structure of a C1C2 chimera where no hydrogen bond between C128 and D156 could be observed (7). The findings either point to structural differences in ChR2 and the chimera or to an influence of the different experimental conditions for crystallization and spectroscopy.

MATERIALS AND METHODS

Point mutations for the E123, C128, and D156 positions were inserted by site-directed mutagenesis in the wild-type (wt) construct of ChR2 comprising the coding region for the amino acids 1–315 of ChR2 and a C-terminal 9x-HisTag. The ChR2 gene was cloned in a pPIC9K vector (Invitrogen, Carlsbad, CA) and used for transformation in *Pichia pastoris*. Cell culture and purification of ChR2 was performed as described in Bamann et al. (14). The buffer of the final product was exchanged by gel filtration and additional dialysis against the buffer required for the experimental respective conditions (e.g., pH4, imidazole-free).

The laser-setup for the time-resolved absorption measurements was described earlier by Huber et al. (23). Briefly, a model No. CPA 2001 laser (Clark MXR, Dexter, MI) delivers femtosecond laser pulses with a central wavelength of 775 nm, operating at a repetition rate of 1 kHz. The wavelength of the pump-pulse was adjusted to the absorption maximum of the sample using a home-built noncollinear optical parametric amplifier. A single-filament white-light continuum was generated by focusing part of the laser fundamental into a sapphire-crystal and used as probe-pulse. This probe pulse was divided into a signal and a reference part and recorded by two 42-segment diode arrays. The time-resolution varied between 50 and 90 fs.

RESULTS

Stationary absorption spectra

In the stationary absorption spectra, the wt clearly exhibits a vibronic fine structure similar to that in NpSRII (10) (Fig. 2 *A*). Three absorption maxima can be identified located at 420 nm, 449 nm, and 474 nm. As reported earlier in ultrafast pump-probe measurements for the wt (10) and for flash-photolysis experiments on C128T (22), the transient data were not affected by changing the excitation wavelength. Therefore, a contribution from several spectrally different states can be ruled out. The absorption

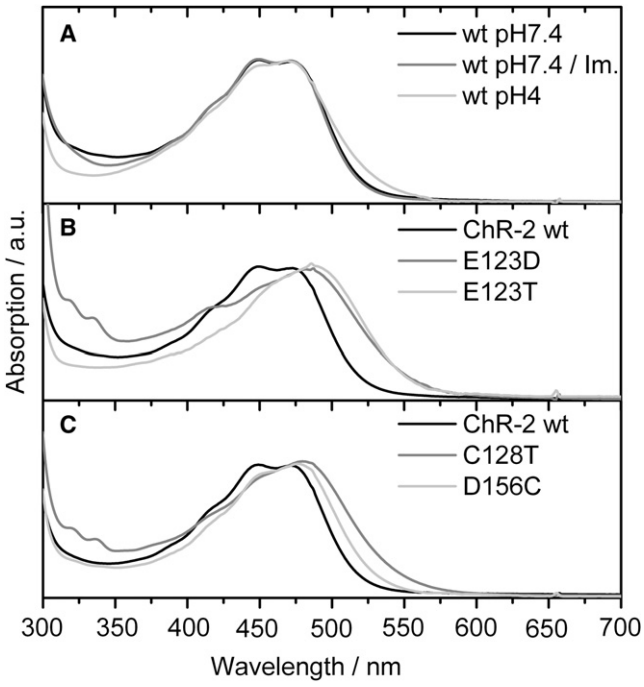

FIGURE 2 Stationary absorption spectra of the measured samples: (*A*) The influence of pH and imidazole (Im.); (*B*) E123D and E123T; and (*C*) C128T and D156C.

spectra for ChR2 wt shows only a weak pH dependence in contrast to the large spectral shift that was reported for ChR1 (24). Similar spectral shifts were also observed for other retinal proteins like bR (25) and proteorhodopsin (26) and were assigned to the protonation state of the primary proton acceptor. The absorption properties of ChR2 are not influenced by imidazole (Fig. 2 *A*). Moreover, Fig. 2 *B* displays the absorption spectra of the E123D and E123T mutants. It is obvious that the vibronic fine structure is less pronounced for the E123D mutant ($\lambda_{max} = 486$ nm) and is nearly absent for E123T ($\lambda_{max} = 490$ nm)). The absorption maxima of both mutants are slightly red-shifted compared to the wt. For the C128T ($\lambda_{max} = 480$ nm) and D156C ($\lambda_{max} = 477$ nm) mutants as well, a slight red-shift of the absorption spectrum is visible and again, the vibronic fine structure is less pronounced but still present in both mutants (Fig. 2 *C*).

Influence of pH and imidazole on the primary photodynamics

Fig. 3 compares the temporal evolution of the ChR2 absorption difference spectrum at different pH and imidazole concentrations after photoexcitation. The overall spectral absorption features are quite similar for all samples. The depopulation of the ground state (GSB) can be observed in the spectral region of the cw-absorption band. At the red-end of the probed spectral range (680–750 nm), a negative difference band indicates the stimulated emission (SE). Obviously, the lifetime of the excited state is affected by pH.

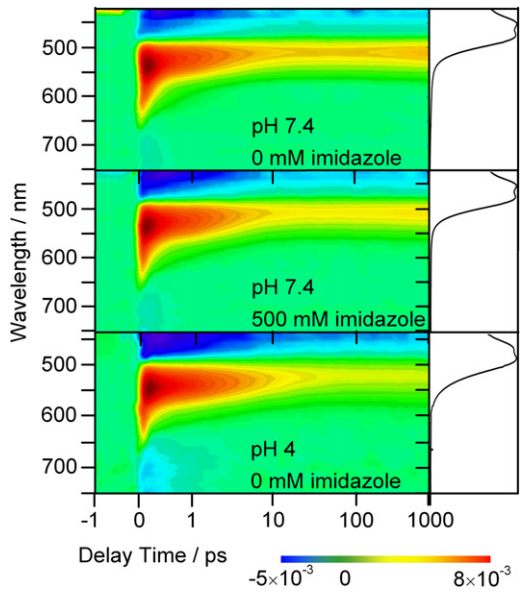

FIGURE 3 Transient absorption changes of ChR2 wt after excitation at 480 nm. The figure is color-coded. (*Blue areas* mark region with negative absorbance changes, *red* with positive, and *green areas* without absorption changes.) The data are plotted linear until 1 ps and logarithmic from 1 ps to 1 ns. For comparison, the absorption spectra are plotted at the right.

This is illustrated by the time constants obtained from global fit analysis that is increased from 2.9 ps to 4.6 ps upon lowering the pH (Table 1). For wavelengths ranging from 500 to 650 nm, a strong positive absorption feature is observed directly after photoexcitation, which is attributed to the excited state absorption (ESA). This positive signal decays on a picosecond-timescale to a constant signal caused by the first ground-state intermediate in the photocycle of ChR2 (K-intermediate) containing the isomerized retinal. For the imidazole-free sample at alkaline conditions, an additional absorption feature can be observed rising at the end of the investigated time range. This data set requires five time constants in the global fit analysis compared to the four that are necessary to approximate the transient data upon addition of imidazole or at pH 4 (Table 1). Nevertheless, the initial photodynamics until 2 ps is not affected by imidazole (see the Supporting Material).

Fig. 4 displays the decay-associated spectra (DAS) of the individual time constants. Because the first time constant is in the same range as the time resolution of our setup, it is not considered further. The spectra of τ_2 exhibit contributions from the decay of GSB, ESA, and SE. Therefore, τ_2 is attributed to the decay of the excited state. In contrast, the spectra of τ_3 do not show any contributions from the stimulated emission at alkaline pH, whereas a small contribution was observed at pH 4 (see *inset*). The τ_3-contributions in the spectral range of the photoproduct describe the decay of a hot early photoproduct. Only at pH 7.4, in the absence of imidazole, is an additional time constant (τ_4) required to satisfactorily describe the transient data. The DAS of τ_4 mainly shows a negative contribution at ~510 nm, which indicates that τ_4 is required only to describe the formation of this additional absorption feature. Moreover, a small positive contribution can be observed at the blue-end of the spectrum, because the GSB band becomes slightly more negative on this timescale. A shift of the λ_{max} of the observed photoproduct may account for these observations. The time constant τ_5 is set to infinite and represents the difference spectrum between the first ground-state intermediate of the photocycle of ChR2 and its ground state. The high similarity of the corresponding DAS of τ_5 indicates

TABLE 1 Transient data were analyzed by global fit analyses

	τ_1/ps	τ_2/ps	τ_3/ps	τ_4/ps	τ_5
wt	<0.1	0.40	2.7	200	Infinite
wt/imidazole	<0.1	0.41	2.9	—	Infinite
wt/pH 4	<0.1	0.33	4.6	—	Infinite
E123D	<0.1	0.12	1.8	—	Infinite
E123T	<0.1	0.72	4.8	—	Infinite
C128T	<0.1	0.30	1.8	69	Infinite
D156C	<0.1	0.32	2.6	—	Infinite

Term "wt" indicates wild-type. A sum of exponential decays with the same time constants but different amplitudes was used to approximate each transient data set. The samples are measured at pH 7.4 without imidazole, otherwise it is remarked in the table.

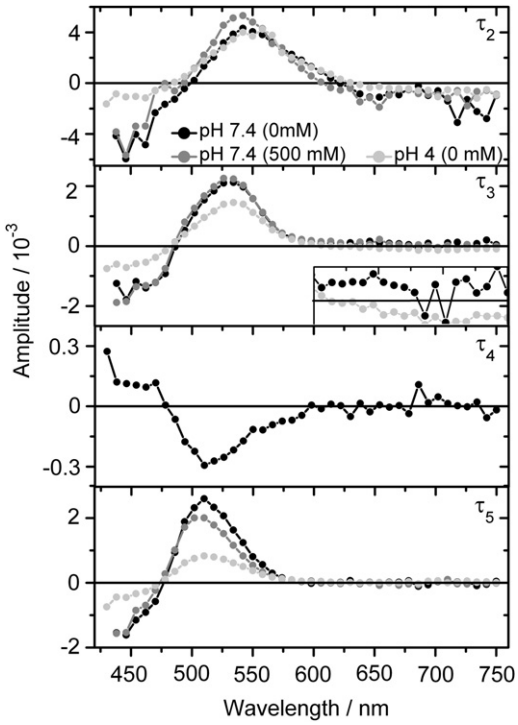

FIGURE 4 Decay-associated spectra (DAS) of the time constants obtained by global fit analysis of the transient data for ChR2 wt at pH 7.4 in the presence and absence of imidazole and for pH 4.

that the absorption spectrum of the first photoproduct is not affected by changing the imidazole concentration or the pH, as for the ground state (Fig. 2).

A negative charge within the retinal binding pocket catalyzes isomerization

If the isomerization kinetics at acidic conditions is slowed down by protonating aspartate and glutamate residues within the retinal binding pocket, a similar effect should be observed by replacing E123 with a neutral amino acid like threonine. In Fig. 5, the transient absorption spectra for the E123T and E123D mutants are presented. The time-resolved spectrum of E123D is similar to the wt (Fig. 3), which is not surprising considering the fact that the functional acid group is conserved. The main difference in the ultrafast dynamics is that the positive absorption feature at ~510 nm for longer delay times is nearly absent. In contrast to this, the introduction of a neutral amino acid in E123T has a strong influence on the primary reaction kinetics. This is most evident in the long wavelength region of the spectrum where a strong and long lasting signal of the stimulated emission is observed (see the Supporting Material). The transient data reveal that the isomerization process is in general slowed down in E123T (Table 1). Neither for E123D nor for E123T can an absorption increase at longer delay times (τ_4) be observed.

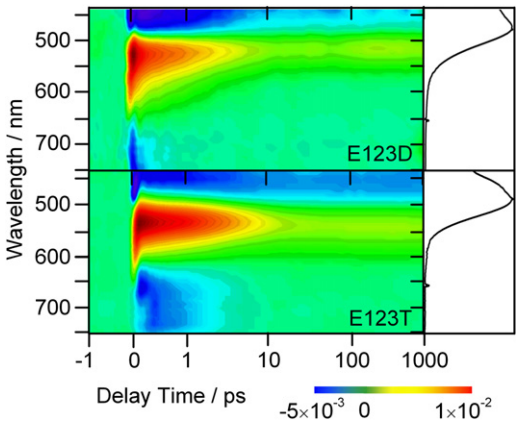

FIGURE 5 Temporal evolution of the absorption changes of the E123D (*top*) and E123T (*bottom*) mutants.

The DAS of τ_2 exhibits contributions from the decay of the ESA and the SE (Fig. 6). Remarkably, no contribution from the recovery of the GSB could be observed for the mutants in contrast to the wt. In the case of E123T and E123D, the DAS of τ_3 exhibits a contribution from the GSB recovery, whereas the other spectral contributions of τ_2 are conserved, although the contribution to the SE for the E123D mutant is quite low. This shows that a biexponential S_1 decay is observed for the E123D and E123T mutants. In contrast to this, the DAS of τ_3 for the wt does not show any contribution from the SE at alkaline pH. The maximum in the DAS of τ_5 for E123T is shifted from 510 nm (wt) to 550 nm. Taking the small spectral red-shift in the absorption spectrum of the ground state into account (15 nm), these findings suggest that the absorption spectrum of the primary photoproduct experiences a stronger red-shift than in wt.

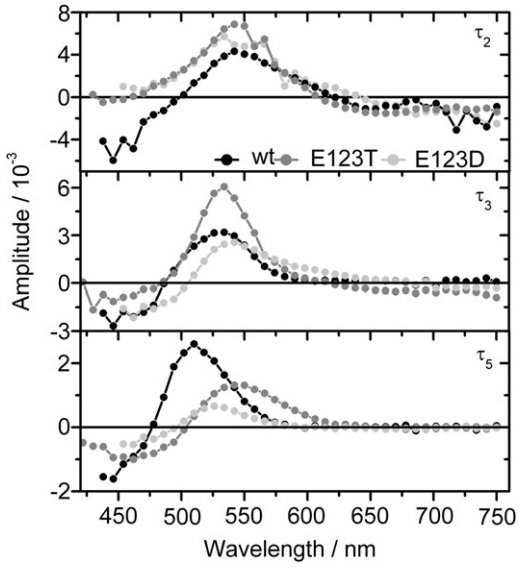

FIGURE 6 DAS of the time constants obtained from global fit analysis of the data sets for E123D and E123T compared to the amplitude spectra obtained for the wt.

Tuning the primary photodynamics of ChR2 by site-specific mutations within the retinal binding pocket (DC-gate)

Previous studies revealed that C128 and D156 play an essential role in channel opening, it was therefore termed "DC-gate" (21). We performed time-resolved absorption measurements on C128T and D156C mutants (Fig. 7). Obviously, the effect of the C128T and D156C mutation on the primary photodynamics differs. In the transient spectra of C128T, one can clearly observe the positive absorption feature at ~510 nm at longer delay times analogous to wt. Interestingly, the time constants obtained by global fit analysis for C128T are smaller than for wt (Table 1). Remarkably, no influence on the decay of the GSB and only slight changes in the decay of the SE could be observed (see the Supporting Material). The DAS reveal that the underlying processes are also affected by the C128T mutation: The DAS of τ_2 and τ_3 contain both contributions originating from the decay of the ESA and the SE, whereas the DAS of τ_3 for the wt exhibits no stimulated emission signal. This indicates a biexponential decay for the C128T mutant compared to a monoexponential decay for the wt. In the DAS of τ_4, a positive contribution at ~560 nm is observed that is absent in wt. The spectral characteristics found in the DAS of τ_4, e.g., a negative amplitude flanked by two positive contributions, can often be attributed to processes, where the bandwidth of the generated photointermediate decreases. The DAS of τ_5 reveals that the absorption maximum of the photoproduct in the case of C128T is more red-shifted than for wt.

In contrast to C128T, the primary photodynamics of D156C resembles the one observed for the wt in the presence of imidazole. No additional absorption feature could be observed at ~510 nm on longer delay times. Because of the high similarity of the time constants depicted in Table 1 and the DAS in Fig. 8, the underlying processes are considered to be similar and are not further discussed.

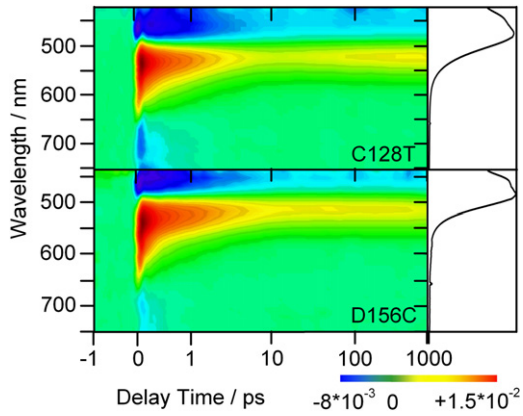

FIGURE 7 Transient absorption spectra of the C128T and D156C mutants excited at $\lambda_{exc.} = 480$ nm.

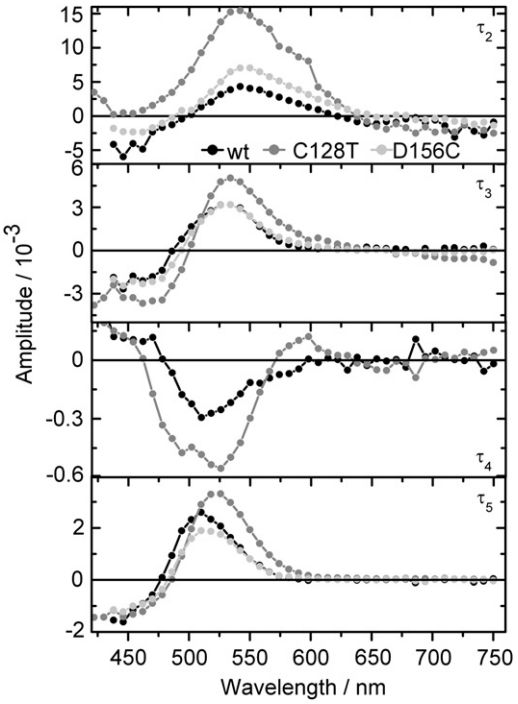

FIGURE 8 DAS of the time constants obtained from global fit analysis for the C128T, D156C, and the wt.

DISCUSSION

Primary reaction of ChR2 at pH 7.4

We present fs-time-resolved absorption measurements on ChR2 wt and several mutants. In this time range the isomerization around the C13-C14 double bond occurs and the first ground-state intermediate in the photocycle is generated. A global fit analysis revealed that five time constants are necessary to satisfactorily describe the transient data. The primary reaction steps for many other retinal proteins like NpSRII (11), and bR (27) can be described in general by four time constants, which correspond to τ_1, τ_2, τ_3, and τ_5 in our study. They are attributed to the following processes: Photon absorption induces a transition into the Franck-Condon region of the excited state (S_1) of the retinal. Subsequently a motion of the initially generated wave packet out of the Franck Condon region occurs (τ_1). The propagation on the potential energy surface of the excited state includes several stretching modes and finally the torsional mode around the C13-C14 double bond leading to the S_1/S_0 conical intersection (τ_2). The time constant τ_2 is in the same range as the decay of an excited-state population that is sometimes termed "J-intermediate" in bR. The existence of this J-intermediate, as well as the question of whether the J-intermediate is an excited (S_1) or a ground state (S_0), are controversially discussed (28–31).

It is supposed that the retinal adopts a highly twisted conformation in this state leading to a close contact of the S_1 and S_0 energy potential surfaces (32). This is in

agreement with theoretical studies investigating the photoisomerization of protonated Schiff bases (33,34). After the subsequent vibrational relaxation of the isomerized photoproduct, the molecule decays, radiationless, on a picosecond timescale to the first ground-state intermediate in the photocycle (that is, red-shifted, with respect to the initial ground state). Low-temperature Fourier transform infrared (FTIR) spectroscopy revealed that this intermediate contains the retinal in its isomerized 13-*cis* conformation (15,35). The quantum yield of photoisomerization is significantly lower than one. This is explained by the fact that the excited retinal either decays to the first K-like intermediate containing the retinal in its isomerized conformation or repopulates its initial all-*trans* ground state (32). This is evident from the DAS of τ_3 that contain contributions for both formation of the photoproduct and repopulation of the ground state.

The DAS of τ_4 shows a negative contribution at ~510 nm as well as a small positive contribution for $\lambda < 470$ nm, indicating a spectral shift of an absorption band. Because at this delay time the first K-like intermediate should be the dominant species, this signature can be attributed to an equilibration between different photointermediates. Upon addition of imidazole, this feature is absent. It is generally accepted that imidazole, like azide, interacts with the hydrogen-bonding network of the protein. For bR, it was shown that azide affects the photocycle dynamics (36–38) or even reestablishes the functionality of the protein after mutation of the primary proton donor D96N (39). Also in NpSRII, azide and imidazole act as weak proton donors, reprotonating the Schiff base during the M-decay in the D75N and F86D NpSRII photocycle (40). Moreover, an accelerated M-decay occurs in the H166A SRI mutant upon addition of imidazole (41), where imidazole leads to the recovery of the SRI functionality. Although the influence of azide and imidazole on the slower photocycle dynamics is well investigated, the knowledge about the influence on the initial steps of the photocycle is sparse. Only for the D75N mutant of NpSRII was an effect of azide on the picosecond-dynamics observed. There, azide induced an additional reaction pathway that was assigned to an accelerated transition between different K-intermediates (42), previously observed in the subsequent photocycle steps of the D75N mutant (43,44).

The existence of several K-intermediates was not only reported for NpSRII. In the photocycle of bR, three different intermediates were reported before L-formation and termed J, K, and KL (45). Although the existence of several K-like-intermediates was controversially discussed (46), other groups using time-resolved absorption (47) and resonance Raman spectroscopy (48) confirmed the appearance of several K-intermediates. Subsequent studies on the early steps of the bR photocycle found two distinct K-intermediates that build up on a timescale of tens of ns (49,50). The equilibration between different K-states is supposed to be accompanied by a relaxation of the twisted chromophore leading to conformational changes in the protein, especially in the microenvironment of the retinal moiety. For bR, the transition between several K-like intermediates is also accompanied by the dislocation of weakly bound water molecules (51). These observations lead to the assumption that similar intermediates could also be present in the photocycle of ChR2. Consequently, the additional absorption feature described by τ_4 is explained by the onset of such a transition between several K-intermediates.

The additional K-intermediate is absent in the presence of imidazole and at acidic pH

The most evident imidazole effect is the disappearance of the additional absorption feature at ~510 nm rising with 200 ps in the imidazole-free sample. The single transient observed at 518 nm (see the Supporting Material) clearly shows that the fast kinetics until 2 ps is not affected by imidazole. Then the transients separate, leading to a slight increase in absorption for the imidazole free sample and to a constant signal for ChR2 with imidazole. Both values and DAS of the first time constants are similar to ChR2 without imidazole, indicating that the underlying processes are identical. Obviously, the isomerization dynamics is not influenced by the addition of imidazole. Interestingly, the additional K-intermediate is also absent at low pH (pH = 4), consequently the picosecond dynamics is not affected by imidazole at pH 4 (data not shown). Apart from a pH and imidazole effect on the hydrogen-bonding network within the retinal binding pocket, a possible charge effect has to be taken into account. Imidazole has a pK_a value of ~7. Therefore, it is positively charged at pH 4, whereas at pH 7.4, the concentration of the neutral species is raised.

A negative point charge within the retinal binding pocket accelerates retinal isomerization

Another effect upon lowering the pH is a slower isomerization rate indicated by an extended lifetime of the excited state (566 nm) and the stimulated emission (750 nm) in Fig. 3. At pH 7.4, D253 and E123 are deprotonated and therefore negatively charged. Lowering the pH presumably leads to a protonation, although the pK_a is hard to determine, due to the weak spectral response of the main absorption band. For E123T, e.g., a neutral amino acid at position E123, the isomerization is clearly retarded. In contrast to this, the primary photodynamics is slightly accelerated for E123D and no additional K-intermediate is observed. This is remarkable because the functional acid group is conserved in E123D, but the lack of the methylene group leads to an altered local geometry and thus to a different interaction of retinal and protein. Moreover, it cannot be ruled out that the hydrogen-bonding network is affected as well, considering the red-shift in the absorption spectra (Fig. 2).

Because the isomerization is faster for wt (pH 7.4) and E123D than for wt (pH 4) and E123T, it is obvious that

a negatively charged amino acid at position E123 is necessary for fast and efficient isomerization. Also for bR it is known that the photoisomerization rate is tremendously reduced due to neutralizing the primary proton acceptor upon D85N mutation (52,53). Furthermore, theoretical studies showed that a negative charge within the retinal binding pocket affects the structure and electronic configuration (54) of the Schiff base and is necessary for a fast photoisomerization (55). These findings can be explained taking the charge-transfer character of the excited state of retinal into account. Upon photoexcitation a change in dipole moment of ~12 D was estimated (56). Because photoexcitation leads to a shift of positive partial charge to the hydrocarbon tail of the retinal (57–59), a negative charge placed in its vicinity catalyzes the isomerization by stabilizing a transition state with a charge-transfer character. Therefore, the negatively charged E123 side chain stabilizes a partial positive charge in the C13-C14 double bond, reduces the double-bond character of this bond and consequently leads to a reduced energetic barrier for isomerization. In addition, it was shown that acetate in the vicinity of the retinal affects the slopes of the S_1 and S_0 surfaces, leading to an earlier crossing of the S_1/S_0 surfaces along the S_1 isomerization path (60).

It should be noted that the underlying reaction processes are also affected by some mutations, leading to a biexponential decay of the excited state compared to a monoexponential decay in the wt. This effect is less pronounced but still present for the E123D mutant. E123D shows the same spectral blue-shift as the wt for longer delay times, indicated by the maximum of the DAS of τ_3 and τ_5 (Fig. 6). In contrast to this, the E123T mutant exhibits a spectral red-shift, suggesting a different K-like intermediate. Interestingly, the DAS of τ_5 for wt at pH 4 and pH 7.4 are identical and therefore indicate that the spectral characteristics of the K-like intermediate are not pH-dependent (Fig. 5). Also, for the absorption spectrum, only a small pH influence could be observed in contrast to the strong red-shift observed in E123T (Fig. 2). The origin of the small red-shift observed in the stationary absorption spectrum for the wt upon acidification is unclear. For Xanthorhodopsin, it was also reported that the absorption spectrum undergoes only a small red-shift upon acidification, which was explained by the assumption that the primary proton acceptor is hydrogen-bonded to a nearby histidine residue (61). However, in ChR2 there is no histidine residue in the vicinity of the primary proton acceptor. These observations thus suggest structural differences in the retinal binding pocket for the E123T mutation that add to the protonation effect of E123 at low pH.

The influence of C128T and D156C point mutation on the primary reaction

The C128T mutant exhibits an accelerated primary reaction, whereas all spectral features observed for the wt are conserved. This is most likely due to changed steric interactions of the retinal with the protein (20). C128 is homologous to T90 in bR that is in van der Waals contact with the retinal (62). The primary reaction for D156C is considerably altered compared to C128T. No additional K-intermediate can be observed. The time constants and DAS are similar to the wt upon addition of imidazole.

As mentioned above, the existence of a hydrogen bond between D156 and C128 is discussed controversially. Whereas FTIR measurements strongly support a hydrogen bond (21), the recently published crystal structure of a C1C2 chimera denies its existence (7). Our data report now a sensitivity of the primary photodynamics toward both aforementioned positions by monitoring the retinal in the visible spectral range. We can only interpret our data with respect to both suggested models. Low-temperature FTIR spectroscopy revealed that the presence of the hydrogen bond between D156 and C128 is preserved upon C128T mutation, although the hydrogen-bond strength is weaker compared to the wt (21). This change in hydrogen-bond strength can also affect the isomerization kinetics. In contrast to this the hydrogen bond is absent in the D156C mutant. Therefore, the hydrogen-bond strength in the ground state influences the kinetics of the excited state decay in addition to steric factors, whereas the presence of this hydrogen bond influences the equilibrium between the different K intermediates.

In the crystal structure of the C1C2 chimera, C128 is supposed to interact with the π-electron system in the retinal, which would explain the altered photoisomerization dynamics upon C128T mutation. However, it remains unclear why the photodynamics in the D156C mutant is similar to the wt, despite the absence of the additional K-intermediate on longer delay times.

CONCLUSIONS

Time-resolved absorption experiments were employed to investigate major determinants of the isomerization process in ChR2. Imidazole was shown to selectively affect the interconversion of several K-intermediates occurring within 200 ps in wt ChR2. This effect can also be reproduced by lowering the pH from 7.4 to 4. The isomerization is slowed down at low pH, which can be understood by taking the polar character of the excited state of the retinal into account. A neutral primary proton acceptor like in E123T leads to an increased lifetime of the excited state; this effect is not observed for E123D, where the negative charge is retained. The results of the pH-dependence as well as the data obtained for E123D and E123T clearly demonstrate the necessity of a negatively charged residue at position 123 for an efficient isomerization. The C128T mutation replacing the cysteine in direct steric contact with the retinal leads to a slight acceleration of the isomerization, which is explained by a changed steric hindrance upon mutation. In contrast, the D156C mutant exhibits isomerization kinetics

like wt in the presence of imidazole, where no additional K-intermediate is observed.

SUPPORTING MATERIAL

Three figures are available at http://www.biophysj.org/biophysj/supplemental/S0006-3495(12)00508-5.

We thank Heike Biehl for excellent technical assistance and Dr. Mirka-Kristin Verhoefen and Dr. Markus Braun for critical reading of the manuscript.

This work has been supported by Deutsche Forschungsgemeinschaft grant SFB 807 "Transport and Communication across Biological Membranes", Cluster of Excellence Frankfurt "Macromolecular Complexes" (J.W. and E.B.), and the Max Planck Society (E.B.).

REFERENCES

1. Nagel, G., D. Ollig, …, P. Hegemann. 2002. Channelrhodopsin-1: a light-gated proton channel in green algae. *Science.* 296:2395–2398.
2. Nagel, G., T. Szellas, …, E. Bamberg. 2003. Channelrhodopsin-2, a directly light-gated cation-selective membrane channel. *Proc. Natl. Acad. Sci. USA.* 100:13940–13945.
3. Feldbauer, K., D. Zimmermann, …, E. Bamberg. 2009. Channelrhodopsin-2 is a leaky proton pump. *Proc. Natl. Acad. Sci. USA.* 106:12317–12322.
4. Boyden, E. S., F. Zhang, …, K. Deisseroth. 2005. Millisecond-timescale, genetically targeted optical control of neural activity. *Nat. Neurosci.* 8:1263–1268.
5. Li, X., D. V. Gutierrez, …, S. Herlitze. 2005. Fast noninvasive activation and inhibition of neural and network activity by vertebrate rhodopsin and green algae channelrhodopsin. *Proc. Natl. Acad. Sci. USA.* 102:17816–17821.
6. Zhang, F., L. P. Wang, …, K. Deisseroth. 2007. Multimodal fast optical interrogation of neural circuitry. *Nature.* 446:633–639.
7. Kato, H. E., F. Zhang, …, O. Nureki. 2012. Crystal structure of the channelrhodopsin light-gated cation channel. *Nature.* 482:369–374.
8. Müller, M., C. Bamann, …, W. Kühlbrandt. 2011. Projection structure of channelrhodopsin-2 at 6 Å resolution by electron crystallography. *J. Mol. Biol.* 414:86–95.
9. Nack, M., I. Radu, …, J. Heberle. 2009. The retinal structure of channelrhodopsin-2 assessed by resonance Raman spectroscopy. *FEBS Lett.* 583:3676–3680.
10. Verhoefen, M. K., C. Bamann, …, J. Wachtveitl. 2010. The photocycle of channelrhodopsin-2: ultrafast reaction dynamics and subsequent reaction steps. *ChemPhysChem.* 11:3113–3122.
11. Lutz, I., A. Sieg, …, W. Zinth. 2001. Primary reactions of sensory rhodopsins. *Proc. Natl. Acad. Sci. USA.* 98:962–967.
12. Polland, H. J., M. A. Franz, …, D. Oesterhelt. 1986. Early picosecond events in the photocycle of bacteriorhodopsin. *Biophys. J.* 49:651–662.
13. Dobler, J., W. Zinth, …, D. Oesterhelt. 1988. Excited-state reaction dynamics of bacteriorhodopsin studied by femtosecond spectroscopy. *Chem. Phys. Lett.* 144:215–220.
14. Bamann, C., T. Kirsch, …, E. Bamberg. 2008. Spectral characteristics of the photocycle of channelrhodopsin-2 and its implication for channel function. *J. Mol. Biol.* 375:686–694.
15. Ritter, E., K. Stehfest, …, F. J. Bartl. 2008. Monitoring light-induced structural changes of channelrhodopsin-2 by UV-visible and Fourier transform infrared spectroscopy. *J. Biol. Chem.* 283:35033–35041.
16. Berndt, A., O. Yizhar, …, K. Deisseroth. 2009. Bi-stable neural state switches. *Nat. Neurosci.* 12:229–234.
17. Berndt, A., P. Schoenenberger, …, T. G. Oertner. 2011. High-efficiency channelrhodopsins for fast neuronal stimulation at low light levels. *Proc. Natl. Acad. Sci. USA.* 108:7595–7600.
18. Cao, Y., G. Váró, …, J. K. Lanyi. 1991. Water is required for proton transfer from aspartate-96 to the bacteriorhodopsin Schiff base. *Biochemistry.* 30:10972–10979.
19. Le Coutre, J., J. Tittor, …, K. Gerwert. 1995. Experimental evidence for hydrogen-bonded network proton transfer in bacteriorhodopsin shown by Fourier-transform infrared spectroscopy using azide as catalyst. *Proc. Natl. Acad. Sci. USA.* 92:4962–4966.
20. Perálvarez-Marín, A., M. Márquez, …, E. Padrós. 2004. Thr-90 plays a vital role in the structure and function of bacteriorhodopsin. *J. Biol. Chem.* 279:16403–16409.
21. Nack, M., I. Radu, …, J. Heberle. 2010. The DC gate in channelrhodopsin-2: crucial hydrogen bonding interaction between C128 and D156. *Photochem. Photobiol. Sci.* 9:194–198.
22. Bamann, C., R. Gueta, …, E. Bamberg. 2010. Structural guidance of the photocycle of channelrhodopsin-2 by an interhelical hydrogen bond. *Biochemistry.* 49:267–278.
23. Huber, R., T. Köhler, …, J. Wachtveitl. 2005. pH-dependent photoisomerization of retinal in proteorhodopsin. *Biochemistry.* 44:1800–1806.
24. Tsunoda, S. P., and P. Hegemann. 2009. Glu 87 of channelrhodopsin-1 causes pH-dependent color tuning and fast photocurrent inactivation. *Photochem. Photobiol.* 85:564–569.
25. Subramaniam, S., T. Marti, and H. G. Khorana. 1990. Protonation state of Asp (Glu)-85 regulates the purple-to-blue transition in bacteriorhodopsin mutants Arg-82-Ala and Asp-85-Glu: the blue form is inactive in proton translocation. *Proc. Natl. Acad. Sci. USA.* 87:1013–1017.
26. Sharaabi, Y., V. Brumfeld, and M. Sheves. 2010. Binding of anions to proteorhodopsin affects the Asp^{97} pK_a. *Biochemistry.* 49:4457–4465.
27. Gai, F., K. C. Hasson, …, P. A. Anfinrud. 1998. Chemical dynamics in proteins: the photoisomerization of retinal in bacteriorhodopsin. *Science.* 279:1886–1891.
28. Hayashi, S., E. Tajkhorshid, and K. Schulten. 2003. Molecular dynamics simulation of bacteriorhodopsin's photoisomerization using ab initio forces for the excited chromophore. *Biophys. J.* 85:1440–1449.
29. Abramczyk, H. 2004. Femtosecond primary events in bacteriorhodopsin and its retinal modified analogs: revision of commonly accepted interpretation of electronic spectra of transient intermediates in the bacteriorhodopsin photocycle. *J. Chem. Phys.* 120:11120–11132.
30. Kobayashi, T., T. Saito, and H. Ohtani. 2001. Real-time spectroscopy of transition states in bacteriorhodopsin during retinal isomerization. *Nature.* 414:531–534.
31. Haupts, U., J. Tittor, and D. Oesterhelt. 1999. Closing in on bacteriorhodopsin: progress in understanding the molecule. *Annu. Rev. Biophys. Biomol. Struct.* 28:367–399.
32. Yabushita, A., and T. Kobayashi. 2009. Primary conformation change in bacteriorhodopsin on photoexcitation. *Biophys. J.* 96:1447–1461.
33. Garavelli, M., T. Vreven, …, M. Olivucci. 1998. Photoisomerization path for a realistic retinal chromophore model: the nonatetraeniminium cation. *J. Am. Chem. Soc.* 120:1285–1288.
34. Schapiro, I., M. N. Ryazantsev, …, M. Olivucci. 2011. The ultrafast photoisomerizations of rhodopsin and bathorhodopsin are modulated by bond length alternation and HOOP driven electronic effects. *J. Am. Chem. Soc.* 133:3354–3364.
35. Radu, I., C. Bamann, …, J. Heberle. 2009. Conformational changes of channelrhodopsin-2. *J. Am. Chem. Soc.* 131:7313–7319.
36. Lakatos, M., G. I. Groma, …, G. Váró. 2002. Characterization of the azide-dependent bacteriorhodopsin-like photocycle of *Salinarum halorhodopsin*. *Biophys. J.* 82:1687–1695.
37. Ormos, P., A. Der, …, Z. Tokaji. 1997. The effect of azide on the photocycle of bacteriorhodopsin. *J. Photochem. Photobiol. B.* 40:111–119.
38. Tittor, J., M. Wahl, …, D. Oesterhelt. 1994. Specific acceleration of deprotonation and reprotonation steps by azide in mutated bacteriorhodopsins. *Biochim. Biophys. Acta.* 1187:191–197.

39. Tittor, J., C. Soell, …, E. Bamberg. 1989. A defective proton pump, point-mutated bacteriorhodopsin Asp^{96}-Asn is fully reactivated by azide. *EMBO J.* 8:3477–3482.

40. Schmies, G., B. Lüttenberg, …, E. Bamberg. 2000. Sensory rhodopsin II from the haloalkaliphilic *Natronobacterium pharaonis*: light-activated proton transfer reactions. *Biophys. J.* 78:967–976.

41. Zhang, X. N., and J. L. Spudich. 1997. His^{166} is critical for active-site proton transfer and phototaxis signaling by sensory rhodopsin I. *Biophys. J.* 73:1516–1523.

42. Verhoefen, M. K., M. O. Lenz, …, J. Wachtveitl. 2009. Primary reaction of sensory rhodopsin II mutant D75N and the influence of azide. *Biochemistry.* 48:9677–9683.

43. Losi, A., A. A. Wegener, …, S. E. Braslavsky. 2000. Aspartate 75 mutation in sensory rhodopsin II from *Natronobacterium pharaonis* does not influence the production of the K-like intermediate, but strongly affects its relaxation pathway. *Biophys. J.* 78:2581–2589.

44. Inoue, K., J. Sasaki, …, M. Terazima. 2007. Laser-induced transient grating analysis of dynamics of interaction between sensory rhodopsin II D75N and the HtrII transducer. *Biophys. J.* 92:2028–2040.

45. Shichida, Y., S. Matuoka, …, T. Yoshizawa. 1983. Absorption-spectra of intermediates of bacteriorhodopsin measured by laser photolysis at room temperatures. *Biochim. Biophys. Acta.* 723:240–246.

46. Yamamoto, N., T. W. Ebbesen, and H. Ohtani. 1994. Does the KL intermediate exist in the photocycle of bacteriorhodopsin? *Chem. Phys. Lett.* 228:61–65.

47. Milder, S. J., and D. S. Kliger. 1988. A time-resolved spectral study of the K and KL intermediates of bacteriorhodopsin. *Biophys. J.* 53:465–468.

48. Doig, S. J., P. J. Reid, and R. A. Mathies. 1991. Picosecond time-resolved resonance Raman-spectroscopy of bacteriorhodopsin-J, bacteriorhodopsin-K, bacteriorhodopsin-KL intermediates. *J. Phys. Chem.* 95:6372–6379.

49. Dioumaev, A. K., and M. S. Braiman. 1997. Two bathointermediates of the bacteriorhodopsin photocycle, distinguished by nanosecond time-resolved FTIR spectroscopy at room temperature. *J. Phys. Chem. B.* 101:1655–1662.

50. Hage, W., M. Kim, …, R. A. Mathies. 1996. Protein dynamics in the bacteriorhodopsin photocycle: a nanosecond step-scan FTIR investigation of the KL to L transition. *J. Phys. Chem.* 100:16026–16033.

51. Dioumaev, A. K., J. M. Wang, and J. K. Lanyi. 2010. Low-temperature FTIR study of multiple K intermediates in the photocycles of bacteriorhodopsin and xanthorhodopsin. *J. Phys. Chem. B.* 114:2920–2931.

52. Song, L., M. A. El-Sayed, and J. K. Lanyi. 1993. Protein catalysis of the retinal subpicosecond photoisomerization in the primary process of bacteriorhodopsin photosynthesis. *Science.* 261:891–894.

53. Logunov, S. L., M. A. ElSayed, …, J. K. Lanyi. 1996. Photoisomerization quantum yield and apparent energy content of the K intermediate in the photocycles of bacteriorhodopsin, its mutants D85N, R82Q, and D212N, and deionized blue bacteriorhodopsin. *J. Phys. Chem.* 100:2391–2398.

54. Tajkhorshid, E., and S. Suhai. 1999. The effect of the protein environment on the structure and charge distribution of the retinal Schiff base in bacteriorhodopsin. *Theor. Chem. Acc.* 101:180–185.

55. Nonella, M. 2000. Electrostatic protein-chromophore interactions promote the all-*trans* → 13-*cis* isomerization of the protonated retinal Schiff base in bacteriorhodopsin: an ab initio CASSCF/MRCI study. *J. Phys. Chem. B.* 104:11379–11388.

56. Schenkl, S., F. van Mourik, …, M. Chergui. 2005. Probing the ultrafast charge translocation of photoexcited retinal in bacteriorhodopsin. *Science.* 309:917–920.

57. Garavelli, M., P. Celani, …, M. Olivucci. 1997. The $C5H6NH2^{+}$ protonated Schiff base: an ab initio minimal model for retinal photoisomerization. *J. Am. Chem. Soc.* 119:6891–6901.

58. Mathies, R., and L. Stryer. 1976. Retinal has a highly dipolar vertically excited singlet state: implications for vision. *Proc. Natl. Acad. Sci. USA.* 73:2169–2173.

59. González-Luque, R., M. Garavelli, …, M. Olivucci. 2000. Computational evidence in favor of a two-state, two-mode model of the retinal chromophore photoisomerization. *Proc. Natl. Acad. Sci. USA.* 97:9379–9384.

60. Cembran, A., F. Bernardi, …, M. Garavelli. 2004. Counterion controlled photoisomerization of retinal chromophore models: a computational investigation. *J. Am. Chem. Soc.* 126:16018–16037.

61. Luecke, H., B. Schobert, …, J. K. Lanyi. 2008. Crystallographic structure of xanthorhodopsin, the light-driven proton pump with a dual chromophore. *Proc. Natl. Acad. Sci. USA.* 105:16561–16565.

62. Kandori, H., N. Kinoshita, …, J. Lugtenburg. 2000. Local and distant protein structural changes on photoisomerization of the retinal in bacteriorhodopsin. *Proc. Natl. Acad. Sci. USA.* 97:4643–4648.